

# Ionic Liquid-Induced Phase-Separated Domains in Lipid Multilayers Probed by X-ray Scattering Studies

Ritika Gupta, Arnab Singh, Velaga Srihari, and Sajal K. Ghosh\*



Cite This: *ACS Omega* 2021, 6, 4977–4987



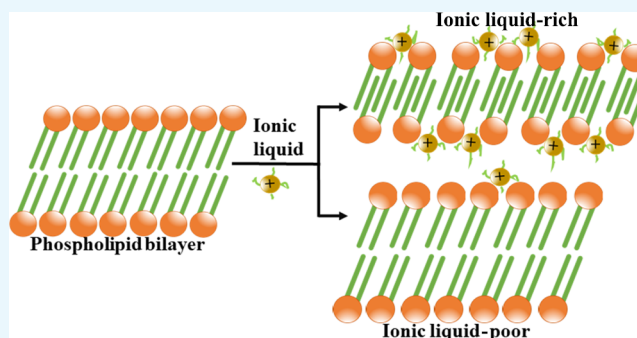
Read Online

ACCESS |

 Metrics & More

 Article Recommendations

**ABSTRACT:** A cellular membrane, primarily a lipid bilayer, surrounds the internal components of a biological cell from the external components. This self-assembled bilayer is known to be perturbed by ionic liquids (ILs) causing malfunctioning of a cellular organism. In the present study, surface-sensitive X-ray scattering techniques have been employed to understand this structural perturbation in a lipid multilayer system formed by a zwitterionic phospholipid, 1,2-dipalmitoyl-*sn*-glycero-3-phosphocholine. The ammonium and phosphonium-based ILs with methanesulfonate anions are observed to induce phase-separated domains in the plane of a bilayer. The lamellar X-ray diffraction peaks suggest these domains to correlate across the bilayers in a smectic liquid crystalline phase. This induced IL-rich lamellar phase has a very low lamellar repeat distance, suggesting the formation of an interdigitated bilayer. The IL-poor phase closely related to the pristine lipid phase shows a decrement in the in-plane chain lattice parameters with a reduced tilt angle. The ammonium and phosphonium-based ILs with a relatively bulky anion, *p*-toluenemethanesulfonate, have shown a similar effect.



## INTRODUCTION

Lipids are organic molecules that are easily soluble in organic solvents but not in water. They include fatty acids, triglycerides, waxes, steroids, terpenoids, and phospholipids. The phospholipids, which are abundant in the plasma membrane, are amphiphilic in nature, having a polar head group and a pair of nonpolar hydrocarbon chains. These molecules are capable of forming different self-assembled structures including monolayers at the air–water interface and bilayers in aqueous solutions.<sup>1</sup> Further, the phospholipids are known to exist in different phases with respect to their chain configuration, of which gel and fluid phases are the commonly observed ones.<sup>2</sup> In the liquid or fluid phase, the hydrocarbon chains are floppy and the effective length of the molecules is shorter in comparison to the gel phase in which the chains are straight and in some cases tilted with respect to the monolayer or bilayer normal.<sup>3–6</sup> These phases in a self-assembled structure can be modified by changing the environment around them by controlling the temperature, pressure, ionic concentration, etc.<sup>3,7,8</sup> The self-assembled bilayer structure of phospholipids in the presence of other membrane components provides an exemplary model of the cellular membrane in order to get insights into their structure and phase behavior.<sup>9–11</sup> Different compositions of lipids, proteins, and cholesterol result in different types of biomembranes. This cellular membrane is responsible for multiple physiological functions such as cell signaling, moderating exocytosis and

endocytosis processes, and cell division.<sup>12</sup> As mentioned above, the external conditions play a vital role in maintaining the membrane structure and dynamics that influence the functioning of the membrane.

Ionic liquids (ILs) are organic salts with a melting point <100 °C which is lower than those of any conventional inorganic salts.<sup>13</sup> Some of them are liquids at room temperature, which are known as room-temperature ILs.<sup>14</sup> A typical IL consists of a cation, which is organic in nature, and an anion, which can be organic or inorganic.<sup>15</sup> These ILs are nonflammable and nonexplosive and have high electrical and thermal conductivities.<sup>16,17</sup> They can be dissolved in organic as well as inorganic solvents.<sup>18</sup> Because of these unique physical and chemical properties, they have a wide range of applications, which have opened up the pathways for the ILs as industrial wastes to have adverse effects on the environment. Recently, it has been observed that the presence of ILs influences the activities of microorganisms, sometimes causing them to die.<sup>19–21</sup> There are reports explaining the toxicity of

Received: December 10, 2020

Accepted: January 28, 2021

Published: February 5, 2021



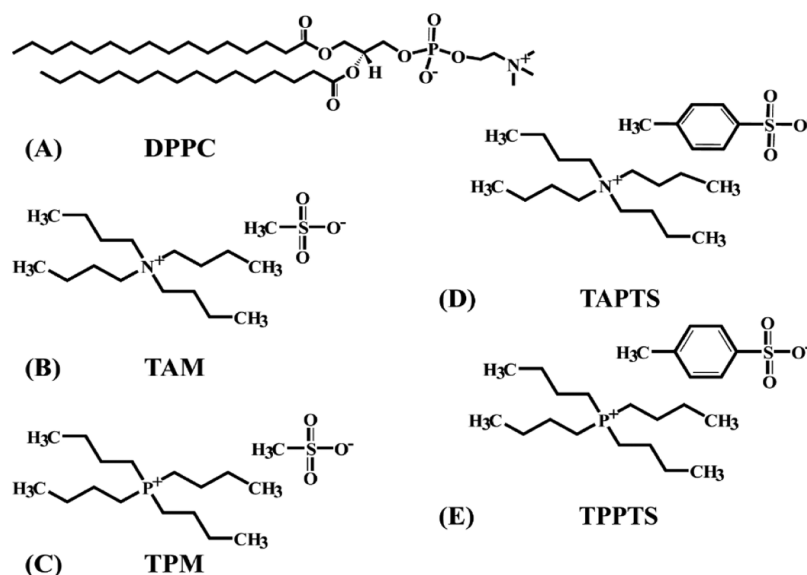


**Figure 1.** Chemical structures of the lipid (A) DPPC and ILs, (B) TAM, (C) TPM, (D) TAPTS, and (E) TPPTS.

these molecules to the environment-friendly bacteria living in soil and water bodies.<sup>19,22</sup> On the other hand, controlled and selective applications of these molecules could be useful to alter the biofunctionality, which may have pharmaceutical importance.<sup>23–25</sup>

Even though the exact molecular mechanism of interactions of ILs with microorganisms is not known, in many cases, the effect is predicted to be related to the restructuring of the cellular membrane.<sup>10,26–28</sup> Therefore, a detailed study of the interaction of ILs with the cellular membrane is an important step to understand the biological activities of these molecules. Note that not only the microorganism but also the human cells are reported to be highly responsive to many of the IL molecules.<sup>29,30</sup> In their recent study, Bakshi et al. have shown that imidazolium-based ILs with long hydrocarbon chains are capable of reducing the growth rate of liver cancerous cells, which is explained to be related to the structural perturbation in the membrane of the cells.<sup>31</sup> Further, the ILs analogous to lipid molecules have shown to be very effective in controlling tumor cells.<sup>32,33</sup> These lipid analogues are also predicted to alter the membrane structure influencing the membrane fluidity depending upon the chain length of the molecules. These reports suggest the potential uses of the IL molecules in pharmaceutical industries.

The structural reorganization of the lipid membrane instigated by ILs can be probed by various X-ray and neutron scattering techniques.<sup>26,34</sup> The X-ray reflectivity study can provide the variation of electron density, interfacial roughness, and thickness of a lipid film from which one can conclude the structural effects of ILs on the lipid membrane.<sup>35,36</sup> The study on a cushioned lipid bilayer has shown that the bilayer thickness of both gel and fluid phases decreases in the presence of ILs, resulting in an increased electron density of the lipid layer.<sup>10</sup> A recent study on the lipid monolayer has suggested this effect to depend on the membrane lateral pressure.<sup>26</sup> The quasi elastic neutron scattering studies on phospholipid vesicles have shown that IL molecules enhance both the lateral and internal motion of lipid molecules, predicting a more flexible two-dimensional (2D) membrane structure where lipid molecules diffuse easily.<sup>34</sup> The solution X-ray diffraction study on multilamellar lipid vesicles (MLVs) has

shown the inter-bilayer spacing to be altered depending on the MLV forming lipid compositions.<sup>11,28</sup> All these studies have provided structural information along the membrane normal, but there is still no description of how the IL could influence the in-plane structure of a membrane. Grazing incidence X-ray diffraction (GIXD) can be used to determine the in-plane crystalline structure of lipid organization and the possible tilt angle of the lipid with respect to the membrane normal.<sup>37–39</sup> Many researchers have utilized this technique to get insights into the 2D arrangement of lipid molecules at the air–water interface as well as on solid-supported lipid multilayers.<sup>40–42</sup> The technique has been adopted here to quantify the effect of different ILs on the in-plane crystalline structure of a zwitterionic phospholipid.

In the present study, 1,2-dipalmitoyl-*sn*-glycero-3-phosphocholine (DPPC) has been used to mimic a plasma membrane. Even though a plasma membrane is a bilayer of lipids, the multilayered samples have been used here to facilitate the X-ray scattering study. To understand the lipid–IL interactions, most of the studies until now have been mainly focused on the imidazolium-based ILs<sup>43–46</sup> and very little attention has been paid to other ILs including ammonium, phosphonium, and pyridinium-based ones.<sup>47,48</sup> It was shown by Stolte et al. that quaternary ammonium salts exhibit drastic toxicity to marine bacteria *Vibrio fischeri* even at lower concentrations compared to many other ILs.<sup>49</sup> The effect was discussed to be linked primarily with the cellular membrane as it is the first target of any foreign molecules to interact. In their report, Kumar and Malhotra have shown the anti-cancer and anti-tumor effects of tetra-substituted ammonium and phosphonium-based ILs, suggesting the observed results to be connected to the altered permeability of the cellular membrane.<sup>50</sup> All these studies lack structural description of the effects of the ILs on the cellular membrane. In the present study, these have been taken into account by applying X-ray scattering techniques.

In the study, four different types of ILs, namely, tetrabutylammonium methanesulfonate (TAM), tetrabutylphosphonium methanesulfonate (TPM), tetrabutylammonium *p*-toluenesulfonate (TAPTS), and tetrabutylphosphonium *p*-toluenesulfonate (TPPTS), are investigated. All these ILs have their melting point ( $T_m$ ) lower than 100 °C.

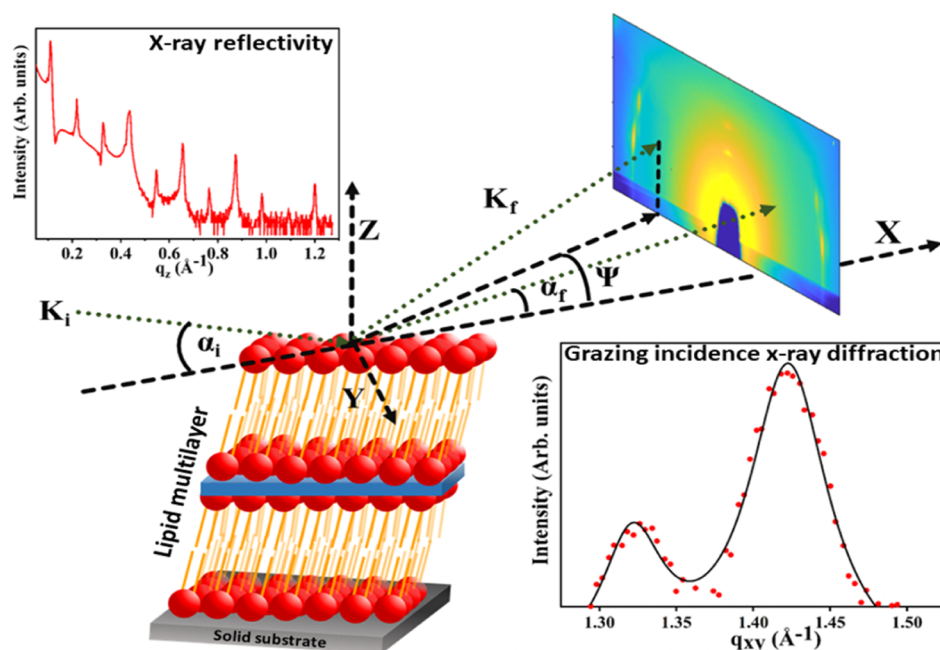


**Figure 2.** Schematic of the X-ray scattering experiment setup for lipid multilayer samples formed on a solid substrate. For *l*-XRD, the specular condition is maintained by keeping angle of incidence ( $\alpha_i$ ) = angle of reflection ( $\alpha_r$ ). For the GIXD, the incident angle is taken to be below the critical angle of the substrate.

Lamellar X-ray diffraction (*l*-XRD) has been employed to probe the structural changes caused by these ammonium and phosphonium-based ILs along the surface normal of the solid-supported lipid multilayers. The grazing incidence measurements have provided information about the in-plane ordering of the lipids in a bilayer.

## MATERIALS AND METHODS

**Materials.** DPPC, TAM ( $T_m \sim 80$  °C), TPM ( $T_m \sim 60$  °C), TAPTS ( $T_m \sim 70$  °C), TPPTS ( $T_m \sim 55$  °C), and chloroform were purchased from Sigma-Aldrich (USA) and were used as received.  $T_m$  refers to the melting temperature of the compounds. All samples were prepared using de-ionized water (resistivity 18 M $\Omega$  cm), and measurements were performed at room temperature. The chemical structures of the lipid and the ILs are shown in Figure 1.

**Formation of Lipid Multilayers.** The DPPC multilayers were prepared on a Si(100) substrate after cleaning the substrate in alternate cycles of bath sonication in methanol and de-ionized water. The substrates were then kept in a UV/ozone chamber for half an hour at 50 °C to hydrophilize the substrate by removing all the organic traces. For a substrate of dimensions of 10 mm  $\times$  15 mm, 40  $\mu$ L of 5 mg/mL chloroform solution of DPPC was spread for the formation of a uniform lipid multilayer. For the DPPC/IL composite system (5, 10, 15, and 20 mol % of the IL in the lipid), a measured volume of the chloroform solution of the IL was mixed with the DPPC solution. After spreading the solution on a substrate, it was kept at rest for 15 min under a laminar flow of air in a hood to let the solvent evaporate slowly. Thereafter, the samples were stored in a vacuum chamber (1 mbar) over a duration of  $\sim$ 12 h for complete evaporation of the organic solvent. For X-ray scattering measurements, these samples were transferred to a sealed chamber having a saturated salt solution of KCl that maintains a constant relative humidity (RH) of 85% in the chamber.

**X-ray Scattering Study.** To investigate the structure of lipid multilayers, two surface-sensitive X-ray scattering techniques, namely, *lamellar (l)*-XRD and GIXD, were used. The *l*-XRD measurements were done using an in-house X-ray setup (Bruker, Discover D8) with a wavelength ( $\lambda$ ) of X-ray photons of 1.54 Å. The scattered photons were collected using a point detector under specular conditions where the angle of incidence ( $\alpha_i$ ) is same as the angle of reflection ( $\alpha_r$ ) (Figure 2). Under these conditions, the scattered intensity is obtained as a function of the  $z$ -component of wave vector transfer ( $q_z$ ). It provides the lamellar repeat distance ( $d$ -spacing) following the Bragg's law,  $q_z = 4\pi/\lambda \sin \alpha_i$ , where  $q_z = 2\pi/d$ . The diffraction peaks are obtained due to smectic liquid crystalline arrangement of lipid bilayers having a thin water layer in between two bilayers.<sup>51</sup> Hence, the  $d$ -spacing is the sum of thicknesses of a lipid bilayer and the water layer.

GIXD measurements were carried out at the Indian Beamline (BL-18B), Photon Factory (PF) (Japan), using X-ray photons of a wavelength of 0.7749 Å with beam dimensions of 0.15 (V) mm  $\times$  1.1 (H) mm. The incident angle ( $\alpha_i$ ) was kept at 0.09°, which is below the critical angle of Si. The scattered photons were collected using a Pilatus 100 K detector having a pixel resolution of 172  $\mu$ m  $\times$  172  $\mu$ m. For this experiment, the shallow incident beam allows to utilize the evanescent wave to probe the lipid multilayers on top of the Si substrate (Figure 2). The sample-to-detector distance was determined by using the diffraction pattern of standard silver behenate. The diffraction data were extracted using the GIXSGUI MATLAB interface.<sup>52</sup> The scattered intensity was then plotted as a function of  $q_{xy}$  and  $q_z$ , exhibiting diffraction peaks related to the in-plane crystalline arrangement of lipid chains.

**Atomic Force Microscopy.** The topography of the multilayer samples on the solid substrate was imaged using an atomic force microscope (XE7, Park System) in the noncontact mode. The atomic force microscopy (AFM) probe

type used was NCHR having a force constant of 40 mN/m. The samples were scanned at a rate of 0.3 Hz, and the image resolution was  $512 \times 512$  pixels with a scan area of  $10 \mu \times 10 \mu$ .

## RESULTS AND DISCUSSION

As the aim of the present study is to comprehend the structural organization of lipid molecules in a membrane in the presence of ILs, two surface-sensitive X-ray scattering techniques have been employed. These nondestructive techniques can provide the structures at a length scale of sub-nanometers to a few nanometers depending upon the wavelength of the X-ray photons.

***l*-XRD Study of Lipid Multilayers.** *l*-XRD is basically the X-ray reflectivity from lipid multilayers. Generally, the terminology “reflectivity” is used for a very thin film with a thickness of a few nanometers where only Kiessig fringes are observed due to interference of scattered X-rays from layers of the sample with varying electron densities along the film normal.<sup>53</sup> In the present case, due to smectic liquid crystalline arrangement of lipid bilayers along the substrate normal, Bragg peaks are observed and, hence, the terminology “diffraction” has been used.<sup>54</sup>

The diffraction data of the pure DPPC multilayer show a set of equidistant diffraction peaks exhibiting a highly oriented stack of lipid bilayers (Figure 3). The lamellar *d*-spacing is

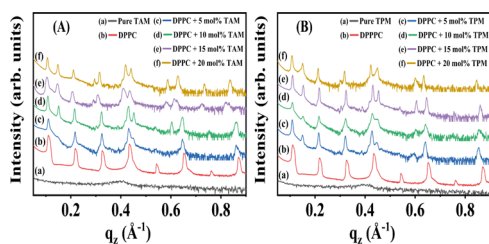


**Figure 3.** Measured diffraction profiles obtained from the *l*-XRD study of lipid multilayers deposited on Si substrates. Data are obtained from pure DPPC multilayers and in the presence of 5, 10, 15, and 20 mol % of (A) TAM and (B) TPM. The measurements were done at room temperature in a sealed chamber to maintain a RH of 85%. The profiles are shifted vertically for clarity.

calculated to be 57.12 Å. This value is a few angstroms less than the reported value for multilamellar vesicles (~63.22 Å) in bulk water where the bilayers can swell apart in aqueous solution due to steric repulsion originating from the out-of-plane thermal fluctuation in the bilayers.<sup>11</sup> For the zwitterionic lipid system, the van der Waals attraction provides the stability.<sup>55</sup> Such a fluctuation is highly restricted in the present

study due to spatial confinement under controlled RH conditions and hence a lesser bilayer spacing.<sup>56,57</sup> The diffraction pattern of the DPPC multilayer in the presence of ammonium-based IL TAM shows another set of diffraction peaks which is identified as a lamellar phase. Therefore, two lamellar phases are found to coexist in the sample. At 5 mol % of the added IL, this new lamellar phase has a spacing of ~41.34 Å, which is much lower than that of the pristine DPPC phase (Table 1). This phase could arise by either layered lamellae of pure ILs or modified lamellae of DPPC with inserted ILs into the bilayers. The first possibility is ruled out as the pure IL is observed to show a broad peak at around  $0.4 \text{ \AA}^{-1}$ , corresponding to a length scale of 15.70 Å (Figure 3A). In the DPPC/TAM mixed system, this broad peak was absent, suggesting the incorporation of the IL in the membrane. The new phase can be designated as 'ionic liquid rich' (IL-rich) phase, while the one close to pure DPPC can be designated as 'ionic liquid poor' (IL-poor) phase. With a higher concentration of the added IL, there is a slight increase in *d*-spacing of both the phases. The IL-rich phase with such a reduced *d*-spacing is probably due to interdigitated arrangement of lipid chains, as reported earlier in other charged lipid systems.<sup>58</sup> This phase may appear in a lipid system with a large head group area<sup>59</sup> or in a mixture of lipids and large ions.<sup>60</sup> The adsorbed ions at the lipid heads provide a greater effective head group area due to electrostatic repulsion between the ions. Further, all the cations of the ILs used in the present study have a 3D structure of a globular shape which is expected to occupy a considerable area at the hydrophobic–hydrophilic interface of the lipid layer. Thereby, it opens up the possibility of chain interdigitation from opposing leaflets within a bilayer. This type of interdigitated lamellar phase may not be observed for rod-like imidazolium-based ILs with a long hydrocarbon chain that spans across a leaflet of the bilayer.

The phosphonium-based IL TPM with the same anion as TAM has exhibited a similar effect on the DPPC multilayer that produces a few diffraction peaks even at the lowest concentration of the added IL (Figure 3B). There is incorporation of the IL in the membrane as the *d*-spacing of the IL-rich phase is calculated to be ~41.89 Å, which is, again, quite low compared to that of the DPPC phase (Table 1). The absence of many other diffraction peaks suggests a modified form factor corresponding to the individual lipid membrane. Even though all the samples have been measured at the same temperature, the structurally different bilayers may exhibit different effects of temperature and thereby differ in their out-of-plane fluctuations and hence the scattering signals. Further, the different *l*-XRD pattern could be due to the disordering effects of the IL molecules. Instead of a simpler methanesulfonate anion, a much bulky *p*-toluenesulfonate anion has been

**Table 1.** Effect of ILs on Inter-Bilayer Spacing (*d*-Spacing) of Multilayers of DPPC<sup>a</sup>

sample	<i>d</i> -spacing (Å)					
	phase 1: IL-poor			phase 2: IL-rich		
	5 mol %	10 mol %	15 mol %	5 mol %	10 mol %	15 mol %
DPPC/TAM	57.12	58.18	59.84	41.34	41.34	42.74
DPPC/TPM	57.64	57.12	57.12	42.74	41.89	41.34
DPPC/TAPTS	57.12	57.12	56.60	41.61	41.34	41.07
DPPC/TPPTS	57.12	57.12	57.64	40.80	40.80	41.07

<sup>a</sup>Phase 1 corresponds to the IL-poor phase closely related to the pristine lipid phase, whereas phase 2 is the IL-rich one. Data are obtained at an RH of 85% at room temperature.

considered to investigate the effects of the size and chemical structure of the anions. For TAPTS and TPPTS, similar diffraction patterns have been observed with a new set of peaks, indicating the existence of the IL-rich interdigitated lamellar phase (Figure 4A,B). Therefore, it is decisive that the ILs with *p*-toluenesulfonate anions have very similar effects to that of the methanesulfonate anion.

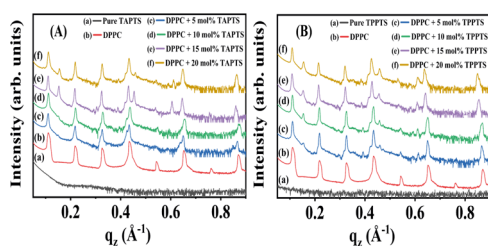


**Figure 4.** Measured diffraction profiles obtained from the *I*-XRD study of lipid multilayers deposited on Si substrates. Data are obtained from pure DPPC multilayers and in the presence of 5, 10, 15, and 20 mol % of (A) TAPTS and (B) TPPTS. The measurements were done at room temperature in a sealed chamber to maintain an RH of 85%. The profiles are shifted vertically for clarity.

The ILs TAM and TPM have methanesulfonate as the anion attached to the hydrophobic cation. In an aqueous solution, the dissociated anions are expected to be in water, while the cations would prefer to be in the membrane. The cationic part of dissociated inorganic salts, such as NaCl and CaCl<sub>2</sub>, is known to adhere to the negatively charged phosphate group of the lipid head due to the electrostatic interaction.<sup>7,61–63</sup> For an

organic salt, such an electrostatic interaction would first lead the cation to adsorb on the membrane surface and then the hydrophobic interaction may pull the ions inside the membrane. Such an insertion of the cations of the ILs would lead to phase-separated domains in the membrane. From the data of TAPTS and TPPTS, it is evident that the anionic part of the ILs does not play any role in affecting the self-assembled structure of the lipid bilayer. The dissociation of the anionic part, however, may increase the entropy of the system to provide the stability. The cations of all the ILs have the same arrangement of the short hydrophobic chains; therefore, the *d*-spacings of the IL-rich phases are observed to be similar.

The new set of diffraction peaks in the presence of the ILs is the signature of phase-separated domains in each bilayer. These domains are then aligned across the bilayer along the substrate normal on which the bilayers are laid. Such an alignment should have a long-range correlation to produce Bragg peaks. There are numerous reports on phase-separated domains in multicomponent lipid systems including the mixtures of saturated and unsaturated lipids of different chain lengths.<sup>64–66</sup> Due to the difference in chain configuration, the saturated lipids form a liquid ordered phase which has a 5–8 Å thicker bilayer compared to the liquid disordered phase formed by the unsaturated lipids in the presence of cholesterol.<sup>67,68</sup> Such a domain is formed to reduce the line tension present at the interface of two lipids due to the hydrophobic mismatch.<sup>69</sup> In the present lipid/IL samples, the interdigitated lamellar phase, with the inserted IL (IL-rich phase), is expected to have a different thickness compared to the pure lipid membrane. There are recent studies performed on a single lipid monolayer and bilayer deposited on a solid

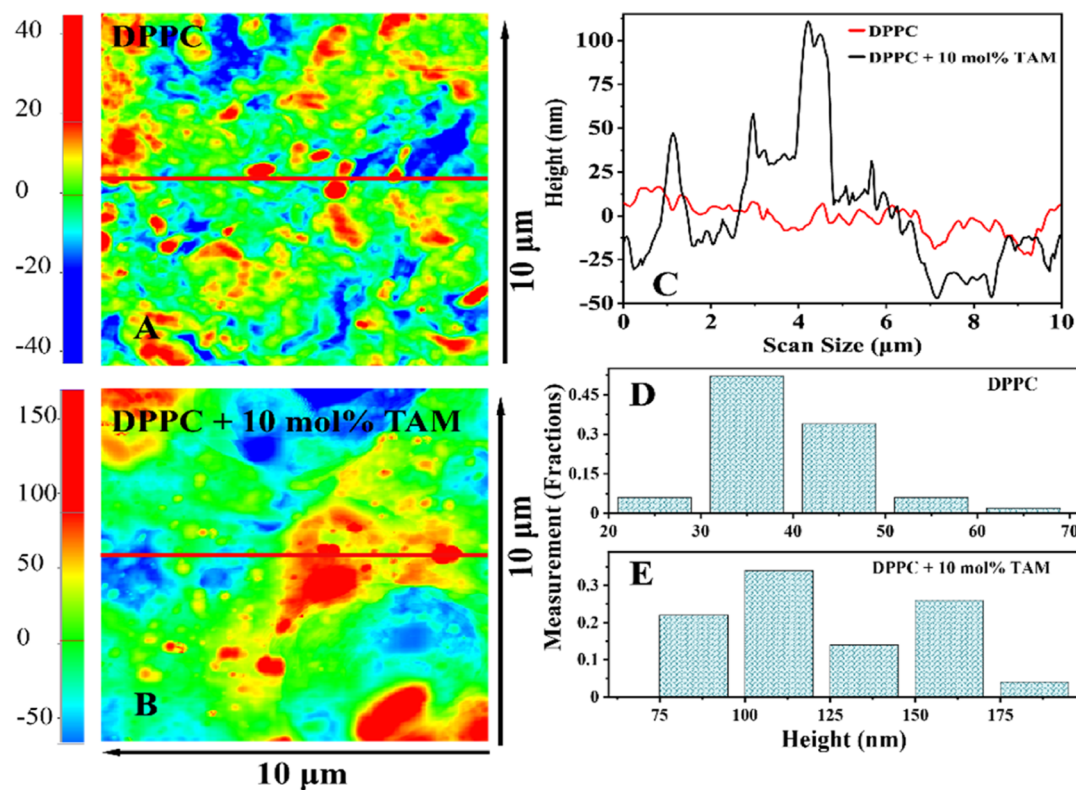


**Figure 5.** AFM images of lipid multilayer samples of (A) pure DPPC and (B) DPPC in the presence of 10 mol % of TAM. (C) Height profiles obtained from the line cuts shown in (A,B). The height distributions shown in (D,E) are obtained from multiple line cuts taken at different regions of multiple samples.

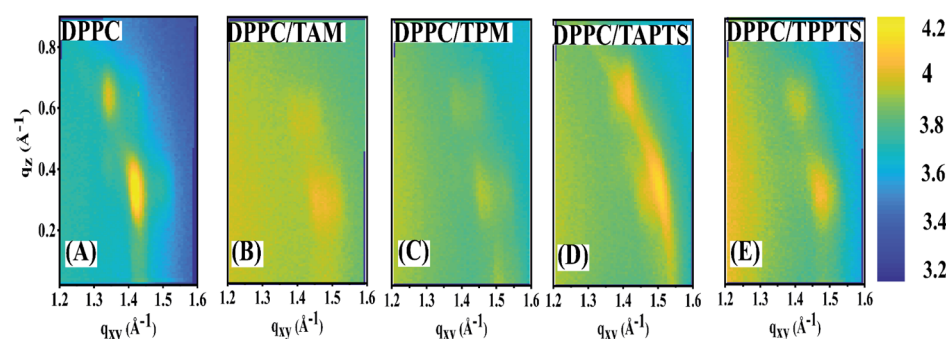


**Figure 6.** 2D GIXD patterns obtained from (A) pure DPPC and added 10 mol % of (B) TAM, (C) TPM, (D) TAPTS, and (E) TPPTS in the DPPC multilayers. The intensities of the images are shown in the log scale.

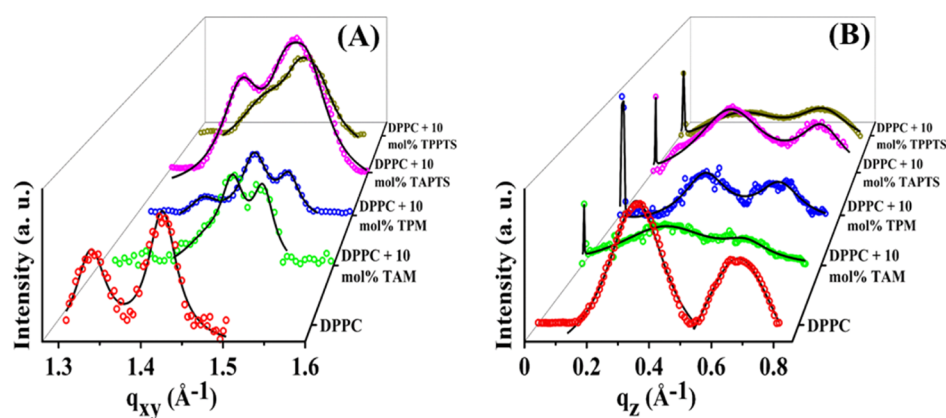


**Figure 7.** GIXD profile from DPPC lipid multilayers in the presence of 10 mol % ammonium and phosphonium-based ILs. Recorded intensity with the variation of  $q_{xy}$  (A) and  $q_z$  (B) with the solid lines representing the Lorentzian fits to the scattered profiles.

surface that show the IL molecules to disorder the lipid chains by inserting themselves into the membrane.<sup>10,26</sup> This insertion occurs due to the hydrophobic interaction between the hydrocarbon chains of lipids and ILs. Due to the random chain, the configurational entropy of the system increases, producing a thinner lipid layer.<sup>9</sup> However, in the present case, the IL-rich phase achieves a thinner lipid bilayer due to interdigitation of chains which would phase-separate out from the pure lipid phase to reduce interfacial line tension. Note that the pure DPPC lipid with saturated chains would form an ordered phase of a higher  $d$ -spacing below its chain melting temperature. In the present study, all measurements were done at room temperature, which is below the reported chain melting temperature of the DPPC lipid ( $\sim 42$  °C).<sup>70</sup>

Under controlled RH conditions, the thin water layer sandwiched between two opposing bilayers has an ordered structure compared to that of the bulk water.<sup>71</sup> In the case of IL-added multilayers, the binding characteristics of water molecules attached to the IL-poor and IL-rich phases would differ as these two phases have differences in their structures and electrostatic nature. Hence, at the interface of IL-poor and IL-rich phases, there will be a mismatch in water networks introducing an energetically unfavorable condition. If the IL-rich domains are aligned across the membrane normal, such interfacial tension would be reduced. Tayebi et al. have provided a similar explanation to out-of-plane correlation of liquid ordered and disordered phases in multicomponent lipid systems in the presence of added cholesterol.<sup>72</sup>

The phase-separated domains correlated across the membrane normal are directly visualized by the patches observed by

imaging the multilayer samples using an atomic force microscope. The smaller patches with a smaller height distribution shown in Figure 5 in the DPPC multilayer sample originate due to the mosaicity in the sample.<sup>73</sup> Note that such a mosaicity does not alter the qualitative results discussed herein. Only the peak positions have been used to figure out the type of 1D periodicity from  $l$ -XRD and the 2D lattice from GIXD (discussed in the following section) where the presence of small domains having the same structure within the domains may not affect the lattice parameters. The bigger patches with a much larger height distribution are observed in the AFM topography of the lipid–IL multilayers, indicating the phase-separated domains in the sample. As explained by Tayebi et al., such a large difference in height is not between only two adjacent lipid bilayers but the cumulative effect of multiple layers across the substrate normal as explained in the section above.<sup>72</sup>

**GIXD Study of Lipid Multilayers.** GIXD is a powerful technique to understand the in-plane organization of lipid molecules in a bilayer.<sup>40,74,75</sup> Here, a highly collimated X-ray beam is allowed to fall on a flat surface below its critical angle to get information about the 2D crystal structure in the surface plane and the possible tilt in lipid molecules with respect to the surface normal. In the GIXD image, out of three components of the momentum transfer vector, only  $q_z$  can be measured separately, and the other two components  $q_x$  and  $q_y$  are related by the expression  $q_{xy} = \sqrt{q_x^2 + q_y^2}$ .<sup>76</sup> This is due to the fact that the domains in the  $x$ – $y$  plane have random orientations and hence behave as the 2D power sample. This technique is

versatile and can be applied for monolayers, bilayers, and multilayer samples.

The set of 2D diffraction patterns obtained from multilayers of pure DPPC and DPPC in the presence of 10 mol % ILs is shown in Figure 6. For the pure DPPC sample, there are two sharp spots positioned at  $q_{xy} > 0$  and  $q_z > 0$ . From these diffraction images, the scattered intensities as a function of  $q_{xy}$  and  $q_z$  were extracted and plotted independently to get the detangled pictures of organization of the lipid molecules in the  $x$ - $y$  plane and the corresponding tilt in the chain. The pure DPPC data were best fitted with two Lorentzian functions to figure out the positions of the peaks. Two peaks were observed at  $q_{xy} = 1.32$  and  $1.41 \text{ \AA}^{-1}$ , which can be indexed as (02) and (11) peaks of a body-centered rectangular lattice, respectively (Figure 6A). The respective lattice parameters are calculated to be  $4.99 \pm 0.01$  and  $9.52 \pm 0.01 \text{ \AA}$ . This lattice can also be explained as the distorted hexagonal lattice, as explained in ref 77. For a pure hexagonal arrangement of lipid molecules without any tilt in the chain, there will be a single degenerate peak. In this case, Bragg rods (the structure factor of the 2D hexagonal lattice) intersect the reciprocal disc (the form factor of the rod-like lipid chain) in such a way that all six first-order diffraction maxima will lie at the same  $q_{xy}$ .<sup>76</sup> The degeneracy is lifted if there is distortion from the ideal hexagonal behavior of the lattice or if there is tilt in the molecule. The tilt of a molecule in the membrane can be quantified from the  $q_z$  positions of peaks. The presence of two peaks, one at  $q_z \sim 0$  and the other at  $q_z > 0$ , suggests the nearest-neighbor (NN) tilt, while the presence of both the peaks for  $q_z > 0$  suggests the next NN (NNN) tilt.<sup>77</sup> The  $q_z > 0$  position of two DPPC peaks at  $0.33$  and  $0.66 \text{ \AA}^{-1}$  as shown in Figure 7B suggests the NNN tilt in the chain. This tilt angle is calculated using  $\tan \theta = K_{nz}/K_{nxy}$  and the value is found to be  $26.56^\circ$ . The NNN tilt observed in this present study in DPPC multilayers differs from the tilt in the DPPC monolayer which is reported to be of the NN type.<sup>63</sup> The organization of lipid chains in a bilayer is decided by the interaction among the lipids of intraleaflet and interleaflets of the bilayer, whereas only intraleaflet lipids influence each other in a monolayer system.

In the presence of ILs, the lipid multilayers have exhibited a modified diffraction pattern with the appearance of a new peak situated close to  $q_z \sim 0$  along with two other peaks at  $q_z > 0$ . The presence of such three peaks is the signature of an in-plane oblique lattice formed by the lipid chains.<sup>76,78,79</sup> The three peaks obtained as a function of  $q_{xy}$  are indexed as (01), (10), and (1-1) of the oblique lattice. The best fit was obtained by using three Lorentzian functions as shown in Figure 7 with the fitted parameters tabulated in Table 2. In the presence of TAM in the DPPC multilayer, the lattice parameters corresponding to this oblique lattice are  $4.83$  ( $a$ ) and  $4.93 \text{ \AA}$  ( $b$ ) with the angle ( $\gamma$ ) between them to be  $117.52^\circ$ . The intermediate tilt between NN and NNN is calculated to be  $22.4^\circ$ , which is smaller than the NNN tilt angle observed in pure DPPC chains. The introduction of all other ILs into the lipid membrane has qualitatively a similar effect, as shown in Figure 7. At this concentration of TPM, the tilt angle is calculated to be  $24^\circ$ , while the angles with TAPTS and TPPTS are observed to be  $26.89$  and  $\sim 24.90^\circ$ .

These GIXD data suggest that the presence of the ILs does not randomize the lipid chain completely; rather, its presence reduces the lattice parameters and tilt angle and hence the effective area of lipid chains. The interdigitated phases observed earlier are found to be gel phases where the lipid

**Table 2. Parameters ( $a$ ,  $b$ ) and the Angle ( $\gamma$ ) between the Lattice Parameters of an Oblique Lattice Formed by the Lipid Chains in the Presence of ILs<sup>a</sup>**

sample	$d_{01}$ (Å)	$d_{10}$ (Å)	$d_{1-1}$ (Å)	$L_{01}$ (Å)	$L_{10}$ (Å)	$L_{1-1}$ (Å)	$a$ (Å)	$b$ (Å)	$\gamma$ (deg)	$\tau$ (deg)
DPPC/10 mol % TAM	$4.39 \pm 0.09$	$4.30 \pm 0.09$	$4.19 \pm 0.05$	$62.83 \pm 3.14$	$141.37 \pm 7.77$	$141.37 \pm 8.48$	$4.83 \pm 0.1$	$4.93 \pm 0.1$	$117.52$	$22.42$
DPPC/15 mol % TAM	$4.65 \pm 0.01$	$4.42 \pm 0.01$	$4.22 \pm 0.01$	$90.62 \pm 8.27$	$62.83 \pm 1.38$	$94.24 \pm 6.49$	$4.91 \pm 0.01$	$5.17 \pm 0.01$	$115.31$	$25.02$
DPPC/10 mol % TPM	$4.55 \pm 0.01$	$4.33 \pm 0.01$	$4.16 \pm 0.01$	$107.92 \pm 5.39$	$117.81 \pm 3.93$	$115 \pm 8.32$	$4.81 \pm 0.01$	$5.05 \pm 0.01$	$115.47$	$24.19$
DPPC/10 mol % TAPTS	$4.49 \pm 0.01$	$4.27 \pm 0.01$	$4.19 \pm 0.01$	$74.40 \pm 5.56$	$70.69 \pm 6.55$	$87 \pm 6.96$	$4.91 \pm 0.01$	$5.16 \pm 0.01$	$119.7$	$26.89$
DPPC/10 mol % TPPTS	$4.49 \pm 0.03$	$4.30 \pm 0.03$	$4.22 \pm 0.03$	$47.92 \pm 2.39$	$83.78 \pm 5.86$	$71.40 \pm 4.28$	$4.83 \pm 0.03$	$5.04 \pm 0.03$	$117.45$	$24.90$

<sup>a</sup>While  $d_{01}$ ,  $d_{10}$ , and  $d_{1-1}$  denote the interplanar spacings,  $L_{01}$ ,  $L_{10}$ , and  $L_{1-1}$  represent the corresponding correlation lengths.  $\tau$  is the tilt angle in the chain.

chains are organized in a 2D crystalline lattice.<sup>58–60</sup> The present results also suggest a similar observation. However, since the in-plane organization of lipids is not long-ranged, the diffraction intensities from IL-poor and IL-rich phases are difficult to separate out as the *d*-spacings are very close to each other.

A lipid bilayer is formed by two monolayers facing each other. Hence, the bilayer thickness is found to be close to twice a monolayer thickness. In the case of interdigitation, the chains of two opposing monolayers penetrate into each other, reducing the bilayer thickness considerably. This is exhibited in the measured *l*-XRD data reflected in the lower *d*-spacing for the IL-rich phase. On the other hand, the GIXD data have shown a decrease in tilt angle, which should have a thickening effect on the bilayer. However, the thinning effect due to the chain interdigitation is much higher than the thickening effect due to the decrease in chain tilt. Hence, an overall thinning effect is observed in the case of the IL-rich phase.

Lipid multilamellar structures are observed in many biological self-assemblies, such as the thylakoid membranes of photosynthetic cyanobacteria or plant chloroplasts, and electrocyte cells in electric eels.<sup>80–82</sup> Even though these natural multilayers are not formed by typical phospholipids, the multilayers of phospholipids have potential applications in nano-biotechnology, especially in the field of biosensors and artificial gene delivery vectors.<sup>83,84</sup> Although there are limitations in following the exact physiological identity, a lipid multilayer is considered as one of the models to comprehend the biophysical behavior of a cellular membrane.<sup>39,85,86</sup> Its planar structure facilitates to use the surface-sensitive scattering techniques such as X-ray reflectivity and GIXD to comprehend the detailed structural organization of lipids in a lipid layer. The physiological membrane consists of multicomponent 2D fluids in which depending upon the chain melting temperature, there are phase-separated domains.<sup>87</sup> These lateral heterogeneities are called “rafts”, and they play very important roles in many cellular processes such as membrane trafficking and cell signalling.<sup>88</sup> It is interesting to observe that the ILs are capable of inducing such a phase-separated domain in a phospholipid bilayer. The majority of the reported results mainly dealt with the ILs of a cylindrical shape that penetrate into the lipid membrane to enhance the chain disorder throughout the bilayer. There is still no study on ILs with a 3D globular shape as those of the present study showing the influence on the in-plane organization of lipid molecules in a membrane. This study is a first one of this kind which may be extended to a complex lipid system in following a physiologically relevant membrane.

The present study was performed with an RH of 85%, which is away from the biologically relevant condition of a higher humidity of 99% or more. It has been reported by Ma et al. that at a higher humidity, the multilayer samples start degrading due to the formation of water droplets on the sample surface.<sup>56</sup> The planar geometry of the sample, which is necessary for the *l*-XRD and GIXD measurements, is defeated in such samples. Further, at a higher humidity, the diffuse scattering signal generated from the out-of-plane fluctuation of a sample interferes with the *l*-XRD and GIXD data. Therefore, the present study was restricted at a lower humidity.

## CONCLUSIONS

The surface-sensitive X-ray scattering studies have proven the phase-separated domains in a lipid bilayer of a saturated

zwitterionic phospholipid. The domains are induced by ammonium and phosphonium-based ILs with the methanesulfonate anion. The effect was also observed in the case of the bulky anion *p*-toluenesulfonate. *l*-XRD has shown that the ILs are absorbed on the lipid head groups causing the formation of the interdigitated bilayer, which phase-separate out from the IL-poor lipid phase with the crystalline chain configuration. The GIXD study has illustrated the chain organization in the presence of these ILs.

The IL–membrane interaction is mostly investigated using the lipid monolayer, the single bilayer on the solid surface, and unilamellar or multilamellar vesicles in aqueous solutions. In the present study, the multilayered structure has been used, which has provided a qualitative description of phase-separated domains in the membrane in the presence of ILs.

## AUTHOR INFORMATION

### Corresponding Author

Sajal K. Ghosh – Department of Physics, School of Natural Sciences, Shiv Nadar University, Tehsil Dadri, Uttar Pradesh 201314, India; [orcid.org/0000-0002-4974-7311](https://orcid.org/0000-0002-4974-7311); Email: [sajal.ghosh@snu.edu.in](mailto:sajal.ghosh@snu.edu.in)

### Authors

Ritika Gupta – Department of Physics, School of Natural Sciences, Shiv Nadar University, Tehsil Dadri, Uttar Pradesh 201314, India; [orcid.org/0000-0002-5814-7756](https://orcid.org/0000-0002-5814-7756)

Arnab Singh – Surface Physics and Material Science Division, Saha Institute of Nuclear Physics, Kolkata 700064, India

Velaga Srihari – High Pressure and Synchrotron Radiation Physics Division, Bhabha Atomic Research Centre, Mumbai 400085, India

Complete contact information is available at: <https://pubs.acs.org/10.1021/acsomega.0c06014>

### Notes

The authors declare no competing financial interest.

## ACKNOWLEDGMENTS

R.G. thanks UGC-DAE CSR (Mumbai Centre) for research fellowship. S.K.G. thanks the Science and Engineering Research Board (SERB), Department of Science and Technology (DST), India, for funding the project (file no. EMR/2016/006221). Preliminary GIXD measurements were done at BL-11, INDUS II, Indore (India). The authors acknowledge DST for financial support and the Saha Institute of Nuclear Physics, Kolkata, and the Jawaharlal Nehru Centre for Advanced Scientific Research, Bangalore, India, for facilitating the experiments at the Indian Beamline, Photon Factory, KEK, Japan. The authors are also thankful to the reviewers for critically reviewing the manuscript, who have enriched the scientific content of the paper.

## REFERENCES

- (1) Ropers, M.-H.; Brezesinski, G. Lipid Ordering in Planar 2D and 3D Model Membranes. *Soft Matter* **2013**, *9*, 9440–9448.
- (2) Feigenson, G. W. Phase Boundaries and Biological Membranes. *Annu. Rev. Biophys. Biomol. Struct.* **2007**, *36*, 63–77.
- (3) Lewis, R. N. A. H.; Mak, N.; McElhaney, R. N. A Differential Scanning Calorimetric Study of the Thermotropic Phase Behavior of Model Membranes Composed of Phosphatidylcholines Containing Linear Saturated Fatty Acyl Chains. *Biochemistry* **1987**, *26*, 6118–6126.

- (4) Stamatoff, J. B.; Graddick, W. F.; Powers, L.; Moncton, D. E. Direct Observation of the Hydrocarbon Chain Tilt Angle in Phospholipid Bilayers. *Biophys. J.* **1979**, *25*, 253–261.
- (5) Tristram-Nagle, S.; Zhang, R.; Suter, R. M.; Worthington, C. R.; Sun, W. J.; Nagle, J. F. Measurement of Chain Tilt Angle in Fully Hydrated Bilayers of Gel Phase Lecithins. *Biophys. J.* **1993**, *64*, 1097–1109.
- (6) Sun, W. J.; Tristram-Nagle, S.; Suter, R. M.; Nagle, J. F. Structure of Gel Phase Saturated Lecithin Bilayers: Temperature and Chain Length Dependence. *Biophys. J.* **1996**, *71*, 885–891.
- (7) Böckmann, R. A.; Grubmüller, H. Multistep Binding of Divalent Cations to Phospholipid Bilayers: A Molecular Dynamics Study. *Angew. Chem., Int. Ed.* **2004**, *43*, 1021–1024.
- (8) Akutsu, H.; Seelig, J. Interaction of metal ions with phosphatidylcholine bilayer membranes. *Biochemistry* **1981**, *20*, 7366–7373.
- (9) Bhattacharya, G.; Mitra, S.; Mandal, P.; Dutta, S.; Giri, R. P.; Ghosh, S. K. Thermodynamics of Interaction of Ionic Liquids with Lipid Monolayer. *Biophys. Rev.* **2018**, *10*, 709–719.
- (10) Bhattacharya, G.; Giri, R. P.; Saxena, H.; Agrawal, V. V.; Gupta, A.; Mukhopadhyay, M. K.; Ghosh, S. K. X-Ray Reflectivity Study of the Interaction of an Imidazolium-Based Ionic Liquid with a Soft Supported Lipid Membrane. *Langmuir* **2017**, *33*, 1295–1304.
- (11) Mitra, S.; Ray, D.; Bhattacharya, G.; Gupta, R.; Sen, D.; Aswal, V. K.; Ghosh, S. K. Probing the Effect of a Room Temperature Ionic Liquid on Phospholipid Membranes in Multilamellar Vesicles. *Eur. Biophys. J.* **2019**, *48*, 119–129.
- (12) Yeagle, P. L. *The Membranes of Cells*; Academic Press, 2016.
- (13) Freemantle, M. *An Introduction to Ionic Liquids*; Royal Society of Chemistry, 2010.
- (14) Hallett, J. P.; Welton, T. Room-Temperature Ionic Liquids: Solvents for Synthesis and Catalysis. 2. *Chem. Rev.* **2011**, *111*, 3508–3576.
- (15) Welton, T. Room-Temperature Ionic Liquids. Solvents for Synthesis and Catalysis. *Chem. Rev.* **1999**, *99*, 2071–2084.
- (16) Valkenburg, M. E. V.; Vaughn, R. L.; Williams, M.; Wilkes, J. S. Thermochemistry of Ionic Liquid Heat-Transfer Fluids. *Thermochim. Acta* **2005**, *425*, 181–188.
- (17) Smiglak, M.; Reichert, W. M.; Holbrey, J. D.; Wilkes, J. S.; Sun, L.; Thrasher, J. S.; Kirichenko, K.; Singh, S.; Katritzky, A. R.; Rogers, R. D. Combustible Ionic Liquids by Design: Is Laboratory Safety Another Ionic Liquid Myth? *Chem. Commun.* **2006**, 2554–2556.
- (18) Canongia Lopes, J. N.; Costa Gomes, M. F.; Pádua, A. A. H. Nonpolar, Polar, and Associating Solutes in Ionic Liquids. *J. Phys. Chem. B* **2006**, *110*, 16816–16818.
- (19) Zhao, D.; Liao, Y.; Zhang, Z. Toxicity of Ionic Liquids. *Clean: Soil, Air, Water* **2007**, *35*, 42–48.
- (20) Samori, C. Ionic Liquids and Their Biological Effects Towards Microorganisms. *Curr. Org. Chem.* **2011**, *15*, 1888–1904.
- (21) Czarny, J.; Piotrowska-Cyplik, A.; Lewicki, A.; Zgoła-Grzeskowiak, A.; Wolko, E.; Galant, N.; Syguda, A.; Cyplik, P. The Toxic Effect of Herbicidal Ionic Liquids on Biogas-Producing Microbial Community. *Int. J. Environ. Res. Public Health* **2019**, *16*, 916.
- (22) Pretti, C.; Chiappe, C.; Pieraccini, D.; Gregori, M.; Abramo, F.; Monni, G.; Intorre, L. Acute Toxicity of Ionic Liquids to the Zebrafish (*Danio Rerio*). *Green Chem.* **2006**, *8*, 238–240.
- (23) Hough, W. L.; Smiglak, M.; Rodríguez, H.; Swatloski, R. P.; Spear, S. K.; Daly, D. T.; Pernak, J.; Grisel, J. E.; Carliss, R. D.; Soutullo, M. D.; Davis, J. H., Jr.; Rogers, R. D. The Third Evolution of Ionic Liquids: Active Pharmaceutical Ingredients. *New J. Chem.* **2007**, *31*, 1429–1436.
- (24) Egorova, K. S.; Gordeev, E. G.; Ananikov, V. P. Biological Activity of Ionic Liquids and Their Application in Pharmaceutics and Medicine. *Chem. Rev.* **2017**, *117*, 7132–7189.
- (25) Stoimenovski, J.; MacFarlane, D. R. Enhanced Membrane Transport of Pharmaceutically Active Protic Ionic Liquids. *Chem. Commun.* **2011**, *47*, 11429–11431.
- (26) Mitra, S.; Das, R.; Singh, A.; Mukhopadhyay, M. K.; Roy, G.; Ghosh, S. K. Surface Activities of a Lipid Analogue Room-Temperature Ionic Liquid and Its Effects on Phospholipid Membrane. *Langmuir* **2019**, *36*, 328–339.
- (27) Evans, K. O. Room-Temperature Ionic Liquid Cations Act as Short-Chain Surfactants and Disintegrate a Phospholipid Bilayer. *Colloids Surf., A* **2006**, *274*, 11–17.
- (28) Jing, B.; Lan, N.; Qiu, J.; Zhu, Y. Interaction of Ionic Liquids with a Lipid Bilayer: A Biophysical Study of Ionic Liquid Cytotoxicity. *J. Phys. Chem. B* **2016**, *120*, 2781–2789.
- (29) Stepnowski, P.; Skladanowski, A. C.; Ludwiczak, A.; Laczyńska, E. Evaluating the Cytotoxicity of Ionic Liquids Using Human Cell Line HeLa. *Hum. Exp. Toxicol.* **2004**, *23*, 513–517.
- (30) Cvjetko, M.; Radošević, K.; Tomica, A.; Slivac, I.; Vorkapić-Furač, J.; Srček, V. Cytotoxic Effects of Imidazolium Ionic Liquids on Fish and Human Cell Lines. *Arch. Ind. Hyg. Toxicol.* **2012**, *63*, 15–20.
- (31) Bakshi, K.; Mitra, S.; Sharma, V. K.; Jayadev, M. S. K.; Sakai, V. G.; Mukhopadhyay, R.; Gupta, A.; Ghosh, S. K. Imidazolium-Based Ionic Liquids Cause Mammalian Cell Death Due to Modulated Structures and Dynamics of Cellular Membrane. *Biochim. Biophys. Acta, Biomembr.* **2020**, *1862*, 183103.
- (32) Wang, D.; Richter, C.; Rühling, A.; Drücker, P.; Siegmund, D.; Metzler-Nolte, N.; Glorius, F.; Galla, H.-J. A Remarkably Simple Class of Imidazolium-Based Lipids and Their Biological Properties. *Chem.—Eur. J.* **2015**, *21*, 15123–15126.
- (33) Wang, D.; Richter, C.; Rühling, A.; Hüwel, S.; Glorius, F.; Galla, H.-J. Anti-Tumor Activity and Cytotoxicity in Vitro of Novel 4,5-Dialkylimidazolium Surfactants. *Biochem. Biophys. Res. Commun.* **2015**, *467*, 1033–1038.
- (34) Sharma, V. K.; Ghosh, S. K.; Mandal, P.; Yamada, T.; Shibata, K.; Mitra, S.; Mukhopadhyay, R. Effects of Ionic Liquids on the Nanoscopic Dynamics and Phase Behaviour of a Phosphatidylcholine Membrane. *Soft Matter* **2017**, *13*, 8969–8979.
- (35) Giri, R. P.; Mukhopadhyay, M. K.; Basak, U. K.; Chakrabarti, A.; Sanyal, M. K.; Runge, B.; Murphy, B. M. Continuous Uptake or Saturation - Investigation of Concentration and Surface-Packing-Specific Hemin Interaction with Lipid Membranes. *J. Phys. Chem. B* **2018**, *122*, 7547–7554.
- (36) Giri, R. P.; Mukhopadhyay, M. K.; Mitra, M.; Chakrabarti, A.; Sanyal, M. K.; Ghosh, S. K.; Bera, S.; Lurio, L. B.; Ma, Y.; Sinha, S. K. Differential Adsorption of a Membrane Skeletal Protein, Spectrin, in Phospholipid Membranes. *Europhys. Lett.* **2017**, *118*, 58002.
- (37) Shih, M. C.; Bohanon, T. M.; Mikrut, J. M.; Zschack, P.; Dutta, P. Pressure and PH Dependence of the Structure of a Fatty Acid Monolayer with Calcium Ions in the Subphase. *J. Chem. Phys.* **1992**, *96*, 1556–1559.
- (38) Durbin, M. K.; Malik, A.; Ghaskadvi, R.; Shih, M. C.; Zschack, P.; Dutta, P. X-Ray Diffraction Study of a Recently Identified Phase Transition in Fatty Acid Langmuir Monolayers. *J. Phys. Chem.* **1994**, *98*, 1753–1755.
- (39) Münster, C.; Lu, J.; Bechinger, B.; Salditt, T. Grazing Incidence X-Ray Diffraction of Highly Aligned Phospholipid Membranes Containing the Antimicrobial Peptide Magainin 2. *Eur. Biophys. J.* **2000**, *28*, 683–8.
- (40) Miller, C. E.; Majewski, J.; Watkins, E. B.; Mulder, D. J.; Gog, T.; Kuhl, T. L. Probing the Local Order of Single Phospholipid Membranes Using Grazing Incidence X-Ray Diffraction. *Phys. Rev. Lett.* **2008**, *100*, 058103.
- (41) Als-Nielsen, J.; Jacquemain, D.; Kjaer, K.; Leveiller, F.; Lahav, M.; Leiserowitz, L. Principles and Applications of Grazing Incidence X-Ray and Neutron Scattering from Ordered Molecular Monolayers at the Air-Water Interface. *Phys. Rep.* **1994**, *246*, 251–313.
- (42) Rauscher, M.; Salditt, T.; Spohn, H. Small-Angle x-Ray Scattering under Grazing Incidence: The Cross Section in the Distorted-Wave Born Approximation. *Phys. Rev. B: Condens. Matter Phys.* **1995**, *52*, 16855–16863.
- (43) Benedetto, A.; Heinrich, F.; Gonzalez, M. A.; Fragneto, G.; Watkins, E.; Ballone, P. Structure and Stability of Phospholipid Bilayers Hydrated by a Room-Temperature Ionic Liquid/Water

Solution: A Neutron Reflectometry Study. *J. Phys. Chem. B* **2014**, *118*, 12192–12206.

(44) Benedetto, A.; Ballone, P. Room-Temperature Ionic Liquids and Biomembranes: Setting the Stage for Applications in Pharmacology, Biomedicine, and Bionanotechnology. *Langmuir* **2018**, *34*, 9579–9597.

(45) Messali, M.; Aouad, M. R.; Ali, A. A.-S.; Rezki, N.; Ben Hadda, T.; Hammouti, B. Synthesis, Characterization, and POM Analysis of Novel Bioactive Imidazolium-Based Ionic Liquids. *Med. Chem. Res.* **2015**, *24*, 1387–1395.

(46) Yoo, B.; Shah, J. K.; Maginn, E. J.; Maginn, J. Amphiphilic Interactions of Ionic Liquids with Lipid Biomembranes: A Molecular Simulation Study. *Soft Matter* **2014**, *10*, 8641–8651.

(47) Dolżonek, J.; Cho, C. W.; Stepnowski, P.; Markiewicz, M.; Thöming, J.; Stolte, S. Membrane Partitioning of Ionic Liquid Cations, Anions and Ion Pairs – Estimating the Bioconcentration Potential of Organic Ions. *Environ. Pollut.* **2017**, *228*, 378–389.

(48) Gonçalves da Silva, A. M. P. S. Interaction of Hydrophobic Ionic Liquids with Lipids in Langmuir Monolayers. *Langmuir* **2018**, *34*, 3797–3805.

(49) Stolte, S.; Arning, J.; Bottin-Weber, U.; Müller, A.; Pitner, W.-R.; Welz-Biermann, U.; Jastorff, B.; Ranke, J. Effects of Different Head Groups and Functionalised Side Chains on the Cytotoxicity of Ionic Liquids. *Green Chem.* **2007**, *9*, 760–767.

(50) Kumar, V.; Malhotra, S. V. Study on the Potential Anti-Cancer Activity of Phosphonium and Ammonium-Based Ionic Liquids. *Bioorg. Med. Chem. Lett.* **2009**, *19*, 4643–4646.

(51) Ghosh, S. K.; Aeffner, S.; Salditt, T. Effect of PIP2 on Bilayer Structure and Phase Behavior of DOPC: An X-Ray Scattering Study. *ChemPhysChem* **2011**, *12*, 2633–2640.

(52) Simbrunner, J.; Hofer, S.; Schrode, B.; Garmshausen, Y.; Hecht, S.; Resel, R.; Salzmann, I. Indexing Grazing-Incidence X-Ray Diffraction Patterns of Thin Films: Lattices of Higher Symmetry. *J. Appl. Crystallogr.* **2019**, *52*, 428–439.

(53) Als-Nielsen, J.; McMorrow, D. *Elements of Modern X-ray Physics*; John Wiley & Sons, 2011.

(54) Ma, Y.; Ghosh, S. K.; DiLena, D. A.; Bera, S.; Lurio, L. B.; Parikh, A. N.; Sinha, S. K. Cholesterol Partition and Condensing Effect in Phase-Separated Ternary Mixture Lipid Multilayers. *Biophys. J.* **2016**, *110*, 1355–1366.

(55) Israelachvili, J. N. *Intermolecular and Surface Forces*; Academic Press, 2011.

(56) Ma, Y.; Ghosh, S. K.; Jiang, Z.; Tristram-Nagle, S.; Lurio, L. B.; Sinha, S. K. Accurate Calibration and Control of Relative Humidity Close to 100% by X-Raying a DOPC Multilayer. *Phys. Chem. Chem. Phys.* **2015**, *17*, 3570–6.

(57) Ma, Y.; Ghosh, S. K.; Bera, S.; Jiang, Z.; Schlepütz, C. M.; Karapetrova, E.; Lurio, L. B.; Sinha, S. K. Anomalous Partitioning of Water in Coexisting Liquid Phases of Lipid Multilayers near 100% Relative Humidity. *Phys. Chem. Chem. Phys.* **2016**, *18*, 1225–123232.

(58) Pabst, G.; Lonez, C.; Vandenbranden, M.; Jestin, J.; Radulescu, A.; Ruysschaert, J.-M.; Gutberlet, T. Stalk-Free Membrane Fusion of Cationic Lipids via an Intdigitated Phase. *Soft Matter* **2012**, *8*, 7243–7249.

(59) Winter, I.; Pabst, G.; Rappolt, M.; Lohner, K. Refined Structure of 1,2-Diacyl-P-O-Ethylphosphatidylcholine Bilayer Membranes. *Chem. Phys. Lipids* **2001**, *112*, 137–150.

(60) Cunningham, B. A.; Quinn, P. J.; Wolfe, D. H.; Tamura-Lis, W.; Lis, L. J.; Kucuk, O.; Westerman, M. P. Real-Time X-Ray Diffraction Study at Different Scan Rates of Phase Transitions for Dipalmitoylphosphatidylcholine in KSCN. *Biochim. Biophys. Acta, Biomembr.* **1995**, *1233*, 68–74.

(61) Casillas-Ituarte, N. N.; Chen, X.; Castada, H.; Allen, H. C. Na<sup>+</sup> and Ca<sup>2+</sup> Effect on the Hydration and Orientation of the Phosphate Group of DPPC at Air-Water and Air-Hydrated Silica Interfaces. *J. Phys. Chem. B* **2010**, *114*, 9485–9495.

(62) Casares, J. J. G.; Camacho, L.; Martín-Romero, M. T.; Cascales, J. J. L. Effect of Na<sup>+</sup> and Ca<sup>2+</sup> Ions on a Lipid Langmuir Monolayer:

An Atomistic Description by Molecular Dynamics Simulations. *ChemPhysChem* **2008**, *9*, 2538–2543.

(63) Ghosh, S. K.; Castorph, S.; Kononov, O.; Salditt, T.; Jahn, R.; Holt, M. Measuring Ca<sup>2+</sup>-Induced Structural Changes in Lipid Monolayers: Implications for Synaptic Vesicle Exocytosis. *Biophys. J.* **2012**, *102*, 1394–1402.

(64) Nováková, E.; Giewekemeyer, K.; Salditt, T. Structure of Two-Component Lipid Membranes on Solid Support: An x-Ray Reflectivity Study. *Phys. Rev. E: Stat., Nonlinear, Soft Matter Phys.* **2006**, *74*, 051911.

(65) Sengupta, K.; Raghunathan, V. A.; Katsaras, J. Structure of the Ripple Phase of Phospholipid Multibilayers. *Phys. Rev. E: Stat., Nonlinear, Soft Matter Phys.* **2003**, *68*, 031710.

(66) Veatch, S. L.; Keller, S. L. Miscibility Phase Diagrams of Giant Vesicles Containing Sphingomyelin. *Phys. Rev. Lett.* **2005**, *94*, 148101.

(67) van Duyl, B. Y.; Ganchev, D.; Chupin, V.; de Kruijff, B.; Killian, J. A. Sphingomyelin Is Much More Effective than Saturated Phosphatidylcholine in Excluding Unsaturated Phosphatidylcholine from Domains Formed with Cholesterol. *FEBS Lett.* **2003**, *547*, 101–106.

(68) Rinia, H. A.; de Kruijff, B. Imaging Domains in Model Membranes with Atomic Force Microscopy. *FEBS Lett.* **2001**, *504*, 194–199.

(69) Kuzmin, P. I.; Akimov, S. A.; Chizmadzhev, Y. A.; Zimmerberg, J.; Cohen, F. S. Line Tension and Interaction Energies of Membrane Rafts Calculated from Lipid Splay and Tilt. *Biophys. J.* **2005**, *88*, 1120–1133.

(70) Grabielle-Madellmont, C.; Perron, R. Calorimetric Studies on Phospholipid–Water Systems: II. Study of Water Behavior. *J. Colloid Interface Sci.* **1983**, *95*, 483–493.

(71) Cheng, J.-X.; Pautot, S.; Weitz, D. A.; Xie, X. S. Ordering of Water Molecules between Phospholipid Bilayers Visualized by Coherent Anti-Stokes Raman Scattering Microscopy. *Proc. Natl. Acad. Sci. U.S.A.* **2003**, *100*, 9826–9830.

(72) Tayebi, L.; Ma, Y.; Vashae, D.; Chen, G.; Sinha, S. K.; Parikh, A. N. Long-Range Interlayer Alignment of Intralayer Domains in Stacked Lipid Bilayers. *Nat. Mater.* **2012**, *11*, 1074–1080.

(73) Mandal, P.; Bhattacharya, G.; Bhattacharyya, A.; Roy, S. S.; Ghosh, S. K. Unravelling the Structural Changes of Phospholipid Membranes in Presence of Graphene Oxide. *Appl. Surf. Sci.* **2021**, *539*, 148252.

(74) Kuhl, T. L.; Majewski, J.; Howes, P. B.; Kjaer, K.; von Nahmen, A.; Lee, K. Y. C.; Ocko, B.; Israelachvili, J. N.; Smith, G. S. Packing Stress Relaxation in Polymer–Lipid Monolayers at the Air–Water Interface: An X-Ray Grazing-Incidence Diffraction and Reflectivity Study. *J. Am. Chem. Soc.* **1999**, *121*, 7682–7688.

(75) Majewski, J.; Kuhl, T. L.; Kjaer, K.; Gerstenberg, M. C.; Als-Nielsen, J.; Israelachvili, J. N.; Smith, G. S. X-Ray Synchrotron Study of Packing and Protrusions of Polymer–Lipid Monolayers at the Air–Water Interface. *J. Am. Chem. Soc.* **1998**, *120*, 1469–1473.

(76) Kaganer, V. M.; Möhwald, H.; Dutta, P. Structure and Phase Transitions in Langmuir Monolayers. *Rev. Mod. Phys.* **1999**, *71*, 779–819.

(77) Lee, K. Y. C.; Gopal, A.; von Nahmen, A.; Zasadzinski, J. A.; Majewski, J.; Smith, G. S.; Howes, P. B.; Kjaer, K. Influence of Palmitic Acid and Hexadecanol on the Phase Transition Temperature and Molecular Packing of Dipalmitoylphosphatidyl-Choline Monolayers at the Air–Water Interface. *J. Chem. Phys.* **2001**, *116*, 774–783.

(78) Behyan, S.; Borozenko, O.; Khan, A.; Faral, M.; Badia, A.; DeWolf, C. Nanoparticle-Induced Structural Changes in Lung Surfactant Membranes: An X-Ray Scattering Study. *Environ. Sci.: Nano* **2018**, *5*, 1218–1230.

(79) de Meijere, K.; Brezesinski, G.; Möhwald, H. Polyelectrolyte Coupling to a Charged Lipid Monolayer. *Macromolecules* **1997**, *30*, 2337–2342.

(80) Bald, D.; Kruijff, J.; Rögner, M. Supramolecular Architecture of Cyanobacterial Thylakoid Membranes: How Is the Phycobilisome Connected with the Photosystems? *Photosynth. Res.* **1996**, *49*, 103–118.

- (81) Keegstra, K.; Cline, K. Protein Import and Routing Systems of Chloroplasts. *Plant Cell* **1999**, *11*, 557–570.
- (82) Powers, L.; Clark, N. A. Preparation of Large Monodomain Phospholipid Bilayer Smectic Liquid Crystals. *Proc. Natl. Acad. Sci. U.S.A.* **1975**, *72*, 840–843.
- (83) Lenhert, S.; Brinkmann, F.; Laue, T.; Walheim, S.; Vannahme, C.; Klinkhammer, S.; Xu, M.; Sekula, S.; Mappes, T.; Schimmel, T.; Fuchs, H. Lipid Multilayer Gratings. *Nat. Nanotechnol.* **2010**, *5*, 275–279.
- (84) Radler, J. O. Structure of DNA-Cationic Liposome Complexes: DNA Intercalation in Multilamellar Membranes in Distinct Interhelical Packing Regimes. *Science* **1997**, *275*, 810–814.
- (85) Hung, W.-C.; Lee, M.-T.; Chen, F.-Y.; Huang, H. W. The Condensing Effect of Cholesterol in Lipid Bilayers. *Biophys. J.* **2007**, *92*, 3960–3967.
- (86) Tristram-Nagle, S.; Liu, Y.; Legleiter, J.; Nagle, J. F. Structure of Gel Phase DMPC Determined by X-Ray Diffraction. *Biophys. J.* **2002**, *83*, 3324–3335.
- (87) Quinn, P. J. A Lipid-Phase Separation Model of Low-Temperature Damage to Biological Membranes. *Cryobiology* **1985**, *22*, 128–146.
- (88) Simons, K.; Ikonen, E. Functional Rafts in Cell Membranes. *Nature* **1997**, *387*, 569–572.